Revisiting the superaromatic stabilization energy as a local aromaticity index for excited states

(article starts on next page)

Journal of Physical Organic Chemistry **WILEY**

Revisiting the superaromatic stabilization energy as a local aromaticity index for excited states

Kjell Jorner[1,2,3]

[1]Department of Chemistry and Chemical Engineering, Chalmers University of Technology, Kemigården 4, Gothenburg, SE-41258, Sweden

[2]Chemical Physics Theory Group, Department of Chemistry, University of Toronto, Toronto, Ontario, M5S 3H6, Canada

[3]Department of Computer Science, University of Toronto, 40 St. George St, Toronto, Ontario, M5S 2E4, Canada

Correspondence

Kjell Jorner, Department of Chemistry and Chemical Engineering, Chalmers University of Technology, Kemigården 4, Gothenburg SE-41258, Sweden.
Email: kjell.jorner@chalmers.se

Abstract

The graph theory of aromaticity is a useful framework for analyzing the aromatic properties of polycyclic aromatic hydrocarbons. We present here the magnetically based superaromatic stabilization energy (m-SSE) as a local aromaticity index and validate it against its topologically based counterpart t-SSE. By comparing to DFT-computed aromaticity indices of triplet state excited polybenzenoid hydrocarbons, we find that semi-quantitative agreement can be reached by using the variable β method to account for bond-length alternation. The m-SSE can further be separated into orbital and circuit contributions to gain insight into the basis of the aromatic properties of individual rings. Fully automated algorithms for calculating both m-SSE and t-SSE are now available in the COULSON package. We envision that these graph theoretical aromaticity indices will be of great use to the community to analyze the local aromaticity of excited states.

KEYWORDS

aromaticity, Baird's rule, computational chemistry, excited states, graph theory

1 | INTRODUCTION

The graph theory of aromaticity was developed independently by Aihara[1] in Japan and by Gutman et al[2] in Croatia, with contributions from many others.[3,4] It was based on previous pioneering work on applying graph methods to Hückel theory,[5] starting perhaps with the famous theorem by Coulson and Rushbrooke[6] on alternant hydrocarbons. The graph theory of aromaticity presents a rapid and relatively accurate way of determining the aromatic stabilization energy of a molecule in the form of the so-called topological resonance energy (TRE). It is applicable also to excited states as shown first by Aihara[7,8] for the aromaticity of thermal and photochemical pericyclic reactions and by Ilić et al[9] for regular annulenes. Later work by Nishina et al[10] also

rationalized excited-state intramolecular proton transfer in terms of aromaticity.

While the TRE is a global property of the whole molecule, chemists are often interested in the local aromaticity or antiaromaticity of individual rings. Aihara[11] therefore developed the bond resonance energy (BRE) to measure the stabilization of individual bonds. The superaromatic stabilization energy (SSE) was first developed as a measure of macrocyclic aromaticity[12] but was later adapted as a local aromaticity index and applied to PAHs and nanographene fragments.[13] The TRE, BRE, and SSE form a family of indices that are based on the topological properties of the molecule through its adjacency matrix (how the atoms are connected). As an alternative to the topological indices, Aihara[14] also developed the magnetically based magnetic resonance energy (MRE)

and m-BRE,[15] as equivalents to TRE and BRE. He also used a magnetic version of the SSE index, m-SSE, to study the aromaticity of macrocycles.[16] These magnetic indices are intimately connected to the ring currents and the diamagnetic susceptibility of the molecule, establishing an often sought link between the magnetic and energetic aspects of aromaticity.[17,18] Importantly, they also allow a breakdown of the total aromatic stabilization to individual orbital and circuit contributions that can be visualized and analyzed.

After the recent death of Aihara in 2018, his methods have been sparsely used. Notable exceptions include studies by Dias[19] and Myrvold et al.[20] We have recently implemented all of Aihara's methods in the COULSON Python package. In connection with the work on this package, we have developed an implementation of the m-SSE for local aromaticity of individual rings. This local m-SSE index finally completes the trio of magnetically based versions of their topological counterparts. m-SSE is found to correlate almost perfectly with the topologically

defined SSE (t-SSE), and its computation is also easy to automate. We show that m-SSE is also applicable to excited states. Structural relaxation can be treated by incorporation of bond-length alternation via the variable β method. This is specially important for excited states due to large bond length changes associated with excitation and potential exciton localization.

2 | THEORY

During the final years of his life, Aihara eloquently summarized his work on the graph theory of aromaticity in two exhaustive review articles, the first one focusing on the topologically based indices[21] and the second one on their magnetic counterparts.[15] For full details of the methods, we refer the reader to these two papers and the monograph by Trinajstić.[22] Below, we only briefly sketch the essential theory. We start with familiar Hückel secular determinant in matrix form (Figure 1A).
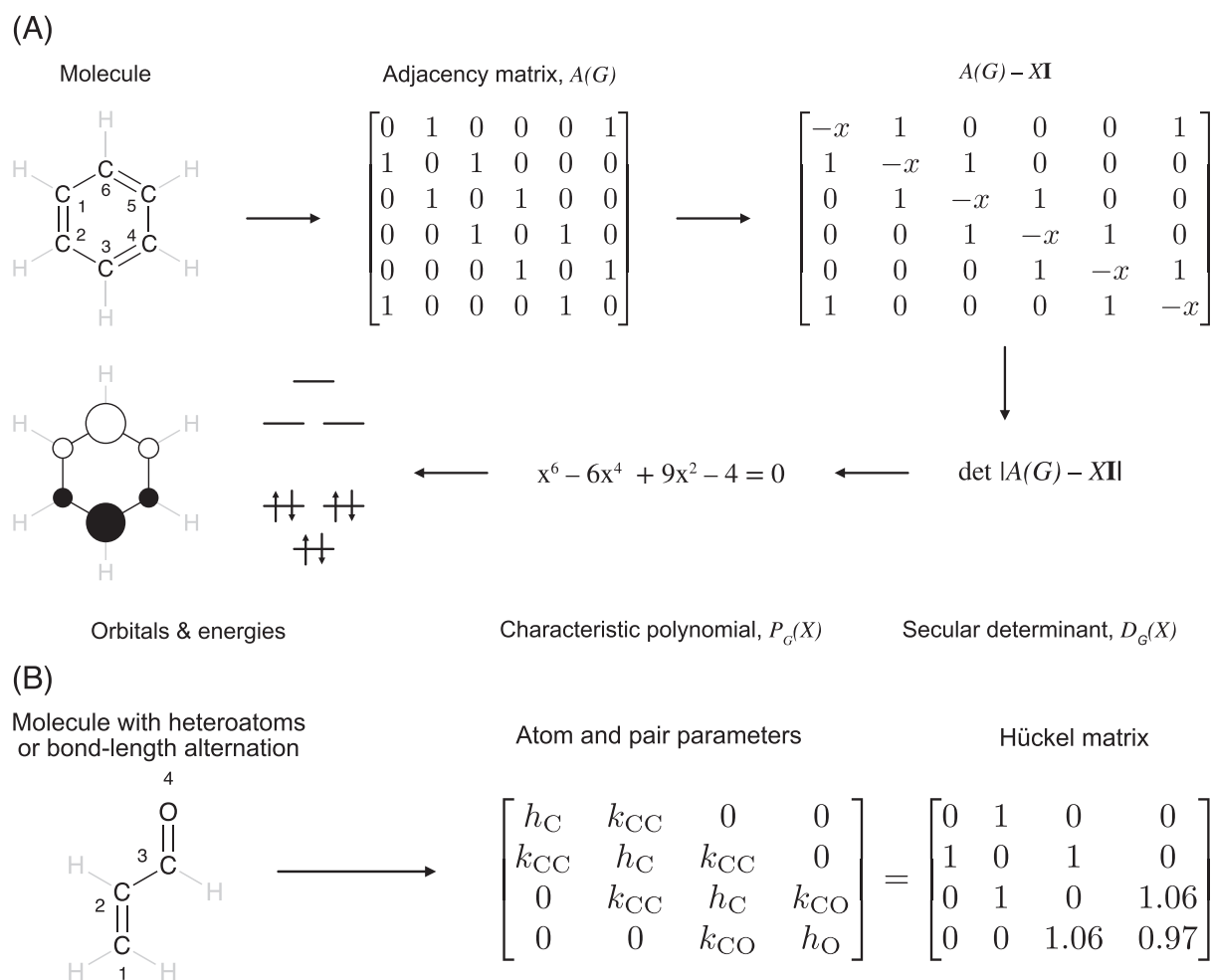

FIGURE 1 (A) Relation between the molecule and its adjacency matrix and the orbitals and their energies in the Hückel molecular orbital theory. (B) Treatment of molecules with heteroatoms and bond-length alternation using atom and pair parameters. The Hückel matrix replaces the adjacency matrix

$$D_G(X) = \det|A(G) - X\mathbf{I}|, \qquad (1)$$

where $A(G)$ is the adjacency (or connectivity) matrix of the molecular graph G, I is the identity matrix, and X is the eigenvalues corresponding to the orbital energies. Expanding this determinant leads to the characteristic polynomial P_G of the graph. To describe heteroatoms or bond-length alternation, $A(G)$ has to be replaced by the so-called Hückel matrix, which uses the parameters h_x and k_{xy} taken from the literature (Figure 1B).[23] This Hückel matrix can be seen as the connectivity matrix of an edge-weighted graph with self-loops for the heteroatoms.[22]

Solving the characteristic polynomial $P_G(X)$ gives the orbital energies X, which multiplied by their associated occupation, numbers, g_i, give the total π-energy of the molecule.

$$E_\pi = \sum_{i=1}^{occ} g_i X_i \qquad (2)$$

To calculate the TRE, we first need to determine the *reference polynomial* R_G. This polynomial defines a purely olefinic reference system and is sometime also called the *acyclic polynomial*. R_G is obtained from P_G by removing all "cyclic" terms in the polynomial. For a detailed discussion of the theory behind this removal, we refer the reader to the monograph by Trinajstić.[22] In brief, the coefficients of P_G can be computed by enumerating subgraphs of the molecular graph, so called Sachs graphs, some of which will feature cycles. R_G is obtained by removing the cyclic subgraphs from the enumeration. In the special case of an all-carbon molecule and $\beta = 1$, it is identical to the *matching polynomial* of the adjacency matrix $A(G)$ known from general graph theory. Solving R_G gives the corresponding orbital energies X^{ref}. For example, for benzene the reference polynomial R_G would

be $x^6 - 6x^4 + 9x^2 - 2$, as compared to P_G, which is $x^6 - 6x^4 + 9x^2 - 4$ (Figure 1A). The energy of the reference system is given by the sum of the orbital energies multiplied by their occupation numbers.

$$E_\pi^{ref} = \sum_{i=1}^{occ} g_i^{ref} X_i^{ref} \qquad (3)$$

The occupation numbers g_i and g_i^{ref} are chosen so as to minimize the π-energy of each system individually.[24] In practice, the reference polynomial is calculated via recursion formulas.[22,25] The topological resonance energy is then given as the difference between the energy of the molecule and its reference.

$$\text{TRE} = E_\pi - E_\pi^{ref} \qquad (4)$$

It should be noted that the reference polynomial does not correspond to any real molecule,[25] except for monocyclic annulenes.[26] The chemical interpretation of its roots as energies is therefore somewhat questionable, although it seems to work empirically.

2.1 | SSE as an aromaticity index for macrocycles and individual rings

The SSE is determined in a similar way as the TRE, but the reference system is different. Here, the reference excludes only the cyclic terms corresponding to the macrocyclic rings, while preserving those from the local rings. The SSE is defined as the total π-energy subtracted by that of the reference system with only local aromaticity.
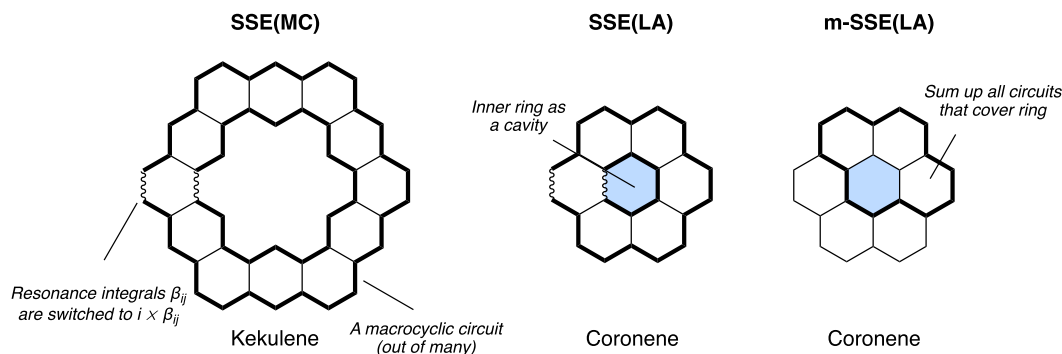
$$\text{SSE} = E_\pi - E_\pi^{loc} \qquad (5)$$

FIGURE 2 Superatomic stabilization energy for macrocyclic conjugation (SSE[MC]), local aromaticity (SSE[LA]), and magnetically based SSE(LA). Wiggly bonds have their corresponding resonance integrals modified. i is the imaginary unit

The SSE was originally invented to measure the "superaromaticity" of molecules like Kekulene, meaning the contributions to the aromatic stabilization due to π-electron circuits that span the whole macrocycle (Figure 2). In practice, it is calculated by a clever manipulation of the elements of the Hückel matrix corresponding to specific bonds.[13]

In 2013, Aihara et al[13] realized that the inner rings in polycyclic systems such as coronene can be seen as small versions of the cavities of large macrocycles like Kekulene (Figure 2). The reference system for the small cavity excludes all the contributions from circuits that surround that ring. Aihara used the term SSE(MC) to refer to the use of SSE when studying macrocyclic conjugation, and SSE(LA) for the use of SSE as a measure of the local aromaticity. In this study, we will exclusively focus on SSE(LA) and therefore drop the extra designation.

A serious caveat with the SSE method is the difficulty to determine which elements of the Hückel matrix to manipulate. We have now developed an automated method that will be reported in a subsequent publication and is used for all calculations in this paper (for the code implementation, see the COULSON package, Section S2 of the supporting information).

2.2 | Magnetically based indices

Following London,[27] Aihara derived the field-dependent magnetic properties of the HMO model in the graph theoretical framework. The central quantity is the so-called circuit resonance energy (CRE), which approximates the contribution to the aromatic stabilization energy of a specific circuit. For the ith circuit, CRE_i (also denoted by A_i in most of Aihara's work) is defined as a sum over the occupied orbitals:

$$CRE_i = A_i = 4 \sum_m^{occ} \frac{P_{G-r_i}(X_m^0)}{P'_G(X_m^0)}.$$ (6)

Here, P_{G-r_i} is the characteristic polynomial of the subgraph of G, where the ring r_i has been removed. P'_G is the derivative of P_G. The superscript for X_m^0 signifies that the eigenvalues are those from a molecule at zero field strength. The eigenvalues are therefore just the regular ones obtained from the characteristic polynomial. In the case of degenerate orbitals and heteroatoms, Equation (6) has to be replaced by a more complicated expression. In particular, higher orders of polynomial derivatives are needed, and in COULSON, we have used the algorithm of Myrvold et al.[20] for this purpose.

The CRE can be used to define linearly additive circuit contributions to the molecular diamagnetic susceptibility,

$$\chi_G = 4.5\chi_0 \sum_i^G A_i \left(\frac{S_i}{S_0}\right)^2,$$ (7)

where χ_0 is the diamagnetic susceptibility of benzene, S_i is the area of circuit i, and S_0 is the area of the benzene ring. The sum runs over all the *simple circuits* in the graph, where a simple circuit is one that does not contain the same atom more than once. The individual circuit contributions to χ_G are given as

$$\chi_i = 4.5\chi_0 A_i \left(\frac{S_i}{S_0}\right)^2.$$ (8)

Analogously, the ring current in the ith circuit is

$$I_i = 4.5 I_0 A_i \frac{S_i}{S_0},$$ (9)

where I_0 is the circuit current for the benzene ring. As noted by Aihara, both χ_G and I have an explicit dependence on the ring area S_i, something that is not often not compensated for when using these magnetic properties as quantitative aromaticity indices.[15] Therefore, the CRE is a more natural choice for measuring the aromaticity of individual rings, regardless of their size.

The magnetic equivalent of the TRE, the MRE, is calculated simply as the sum of the CREs of all the rings in the graph G.

$$MRE_G = \sum_i^{r_i \in G} CRE_i$$ (10)

m-BRE is calculated by summing the contributions of all the circuits containing the bond B in question.

$$m\text{-}BRE_B = \sum_i^{r_i \ni B} CRE_i$$ (11)

Compared to their topological counterparts, the magnetic indices have one serious limitation in that they cannot be computed for open shells with non-integer average occupation numbers that do not match their multiplicity (Figure 3).[28] The physical reasoning underlying this heuristic is that the vanishing orbital energy gap would lead to infinite paramagnetism due to magnetic dipole transitions.[29,30] However, due to the Pauli exclusion principle, if

FIGURE 3 Electronic occupation criteria for calculation of magnetically based properties

$$m\text{-SSE} = \text{MRE} - \text{MRE}_{\text{ref}} \quad (12)$$

the degenerate orbitals in question are occupied with electrons of the same spin, then the magnetic dipole transitions between them are forbidden and the infinite paramagnetism avoided.[28] In fact, the algorithm by Myrvold et al[20] that we are using requires that the high-spin state is calculated. For example, triplet benzene would have three electrons in a shell with twofold degenerate orbitals and one electron in a twofold degenerate shell (Figure 3). The average occupation of each shell is 1.5 and 0.5, respectively. Transitions between the degenerate orbitals are allowed and infinite paramagnetism would result. Another type of system that does not work is D_{4h} cyclobutadiene in the singlet state, which has two unpaired electrons in two degenerate orbitals. The shell of degenerate orbitals would have an average occupation number of 1.0, which is acceptable. But it has two unpaired electrons, which is different from the expected zero unpaired electrons for a (closed-shell) singlet system. On the other hand, triplet cyclobutadiene would work well as the two unpaired electrons are expected for a triplet.

2.3 | m-SSE as a magnetically based local aromaticity index

While defining the SSE as a local aromaticity index for PAHs, Aihara noted that the SSE could in principle be calculated as the sum of the CRE values of all the circuits that surround the ring in question (Figure 2).[13] He even gave an example calculation for coronene but did not further explore the idea or give any details of the calculation. However, the procedure was used as an alternative to SSE(MC) in other work.[16] Similarly to SSE, we have to assume that the calculation of m-SSE was based on a visual selection of all the circuits. In analogy with SSE, m-SSE can be defined as the total MRE of the system minus that of a reference.

MRE_{ref} is the sum of the CREs of the circuits that *do not* surround the ring in question. To facilitate the calculation of m-SSE, we have developed two alternative algorithms that automate the calculation of MRE_{ref}. They will be described in more detail in a future publication, but are outlined in Section S1 of the Supporting Information.

All methods are implemented in the open source COULSON package, which is freely available at https://github.com/kjelljorner/coulson under a permissive MIT license. All the work presented in this paper has been done using Jupyter Notebooks (which are available at https://doi.org/10.5281/zenodo.6965237). It is our hope that COULSON will become a valuable tool for studying aromaticity and that these notebooks can serve as tutorials also for experimentalists wanting to apply the methods.

3 | RESULTS AND DISCUSSION

To clearly distinguish between the topologically based SSE and the magnetically based SSE, we will use the abbreviations t-SSE and m-SSE, respectively. We set out to

1. Validate m-SSE as a local aromaticity index for the ground state by comparison to the well-established t-SSE.
2. Validate m-SSE and t-SSE as local aromaticity indices for the excited state by comparing to results from density functional theory (DFT).
3. Study the effect of bond-length alternation on m-SSE and t-SSE via the variable β method.
4. Analyze the m-SSE in terms of orbital and circuit contributions.

3.1 | Validating m-SSE against t-SSE

To validate m-SSE against t-SSE, we revisited a series of compounds that Aihara used for his original study on t-SSE.[13] The m-SSE and t-SSE values for compounds **1–28** are given in Figure 4. The correlation between the values is given in Figure 5A and is almost perfect with $R^2 = 0.996$. This good correlation is similar to that between MRE versus TRE, and m-BRE versus BRE for benzenoid compounds.[15] The correlation has been shown to be considerably worse for negative SSE values, with MRE exaggerating the antiaromatic character compared to TRE.[15] We therefore also computed a series of neutral and charged non-benzenoid compounds (**29–47**) with low or negative t-SSE values (Figure S2).[15] The results indeed show the expected overestimation also for m-SSE, resulting in a lower R^2 of 0.707 (Figure 5B, blue markers).

Aihara showed that introducing bond-length alternation reduced the exaggeration for low MRE values as compared to TRE.[28] To investigate whether this also applies to m-SSE, we optimized the non-benzenoid molecules with the GFN2-xTB method,[31] constraining them to planar geometries. The GFN2-xTB method is a semi-empirical method based on the extended tight binding (xTB) framework and parametrized to reproduce geometries, frequencies and non-covalent interactions.[32] We then used the variable β method, in the Hückel-Longuet-Higgins-Salem formulation,[33] using the parameters developed by Stolarczyk and Krygowski.[34] Here, the β parameter depends on the bond length r according to the formula

$$\beta = 1 - e^{-(r-r_{ref})/y}, \tag{13}$$

where $r_{ref} = 1.397\text{Å}$ and $y = 0.2756\text{Å}$. The changed β values will lead to different results both for m-SSE and SSE. Using the GFN2-xTB-optimized geometries and the corresponding βs, we recalculated the m-SSE and SSE values (Figure S2). As can be seen from Figure 5B, the correlation is much improved with R^2 going from 0.763 with $\beta = 1$ to 0.995 with a variable β. In particular, the m-SSE values are more positive, as the bond-length alternation in the optimized geometries relieves some of the antiaromaticity.

3.2 | SSE in the triplet state

How does the SSE work as a local aromaticity index in the T_1 state? To answer this question, we looked at a dataset of *cata*-condensed polybenzenoid hydrocarbons

(PBHs) generated by Gershoni-Poranne and co-workers.[35] The DFT-computed quantities include the total spin density per ring (TSDR) and the $NICS_{zz}$ values calculated 1.7 Å above the molecular plane ($NICS_{zz}(1.7)$) as a measure of local aromaticity.

We first compare the TSDRs calculated at the HMO level of theory to those from DFT (Figure 6A) to get an indication if the overall electronic structure is well described. For excited states, exciton localization can be expected to lead to locally distorted bond lengths that deviate from the ideal situation with $\beta = 1$. Indeed, we find a much better correlation with the variable β method based on the DFT geometries. The correlation between t-SSE and m-SSE is also much better (Figure 6B), as seen above also for the non-benzenoid molecules (Figure 5B). Finally, it seems that m-SSE works as a local aromaticity index due to the semi-quantitative correlation with NICS ($R^2 = 0.807$, Figure 6C).

For reference, we also computed the m-SSE and t-SSE values of compounds **1–28** in T_1 using $\beta = 1$ (Figure S1), although it is clear from the preceding discussion that these values should be taken with a pinch of salt. As the benzenoid compounds become antiaromatic in T_1, the correlation between m-SSE and t-SSE suffers (Figure S3a) in a similar way as that for the non-benzenoid compounds in the S_0 state (Figure 5B). The values would rather correspond to vertically excited T_1 states without the alleviation of antiaromaticity due to geometry relaxation. We also computed the non-benzenoid compounds **29–39** & **41–47** (Figure S3b), showing a significant improvement in the correlation between t-SSE and m-SSE when going from $\beta = 1$ ($R^2 = 0.689$) to a variable β ($R^2 = 0.859$). For a discussion of why **40** was excluded, see Section S3. Overall, the correlation remains worse than for the S_0 state.

3.3 | Interpretation of m-SSE

m-SSE has a clear advantage over t-SSE in that it can be broken down into contributions with respect to circuits and orbitals. For a particular ring, we can see which circuits contribute to the aromaticity or antiaromaticity of that ring. This is especially useful for the excited state, where there are only a handful of tools for analyzing local aromaticity. We decided to study a series of compounds known to comply with both Clar's and Baird's rules in the T_1 excited state (Figure 7).[36] The molecules feature a central ring with either 4 or 8 atoms, and we denote them **CB-CBD**, **CB-pen**, and **CB-COT** as they are Clar-Baird (CB) derivatives of the parent cyclobutadiene (CBD), pentalene (pen), and cyclooctatetraene (COT), respectively. In S_0, the central rings are antiaromatic in
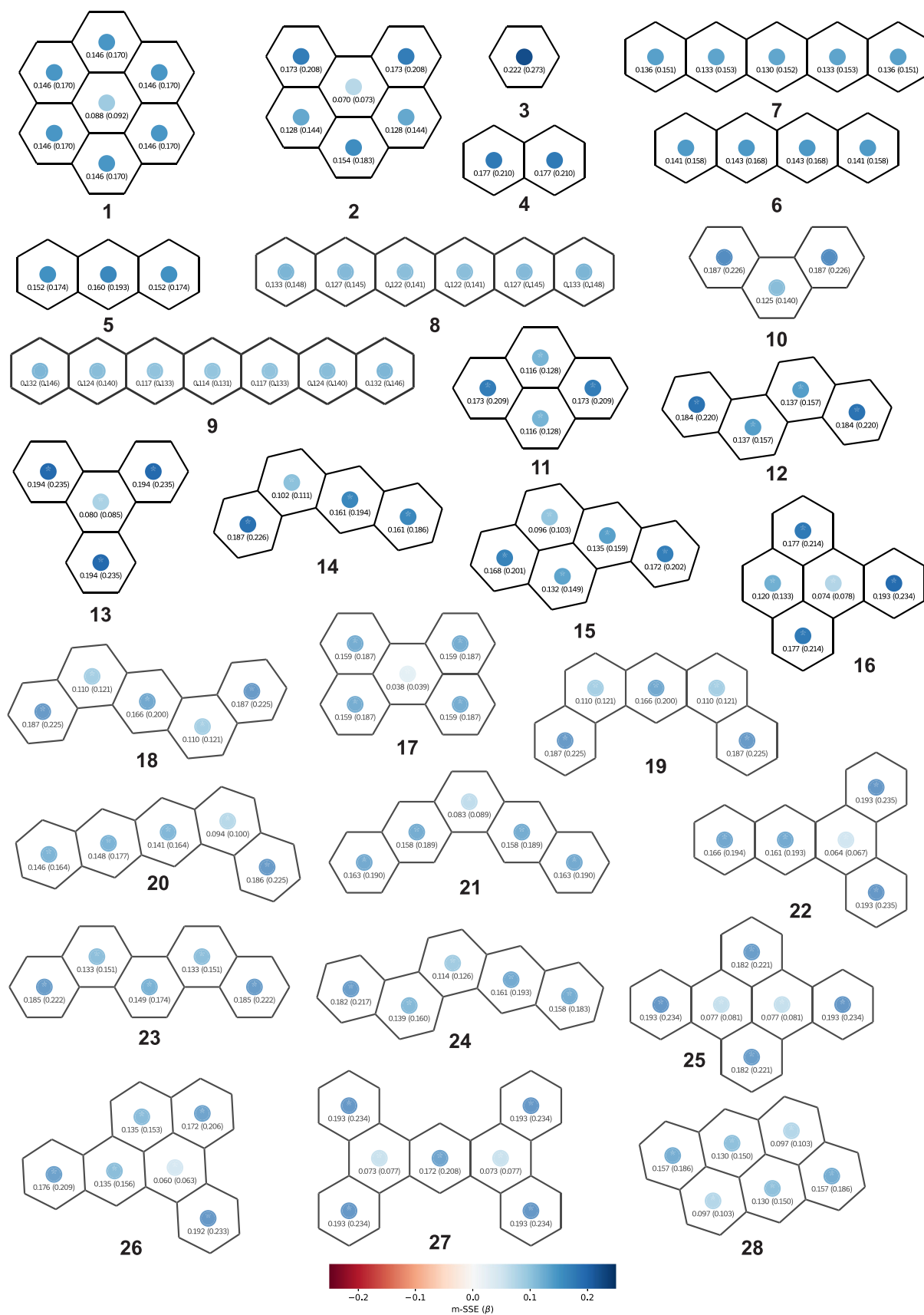
FIGURE 4 Comparison of m-SSE and t-SSE for **1–28** (t-SSE in parenthesis). Colored blue circles indicate the m-SSE values (darker = higher value)
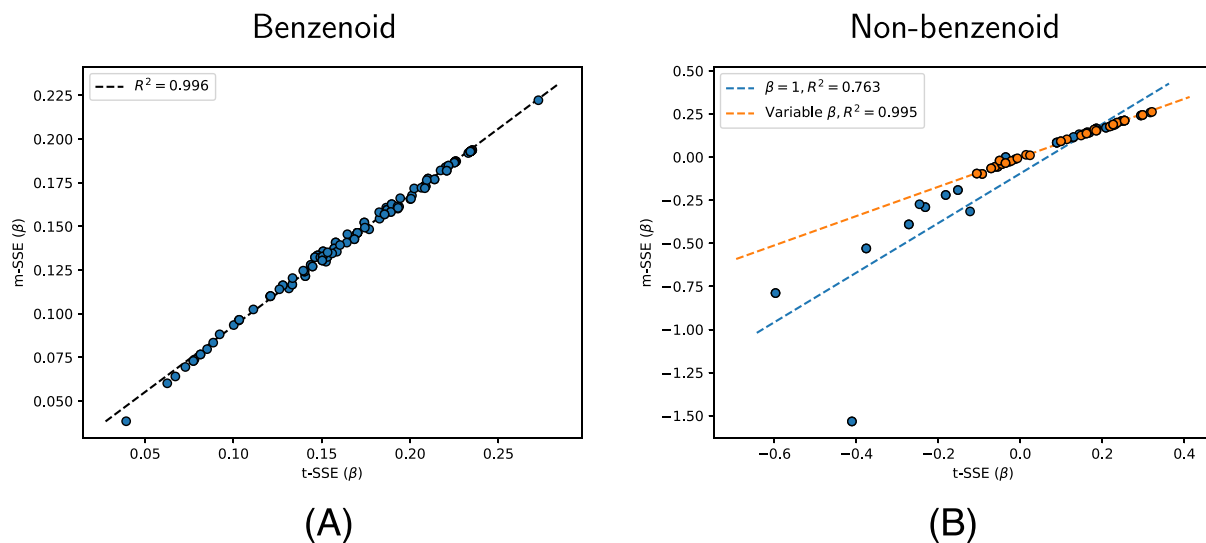
FIGURE 5 Correlation between m-SSE and t-SSE for (A) benzenoid molecules **1–28** and (B) non-benzenoid molecules **29–47**, with and without variable β
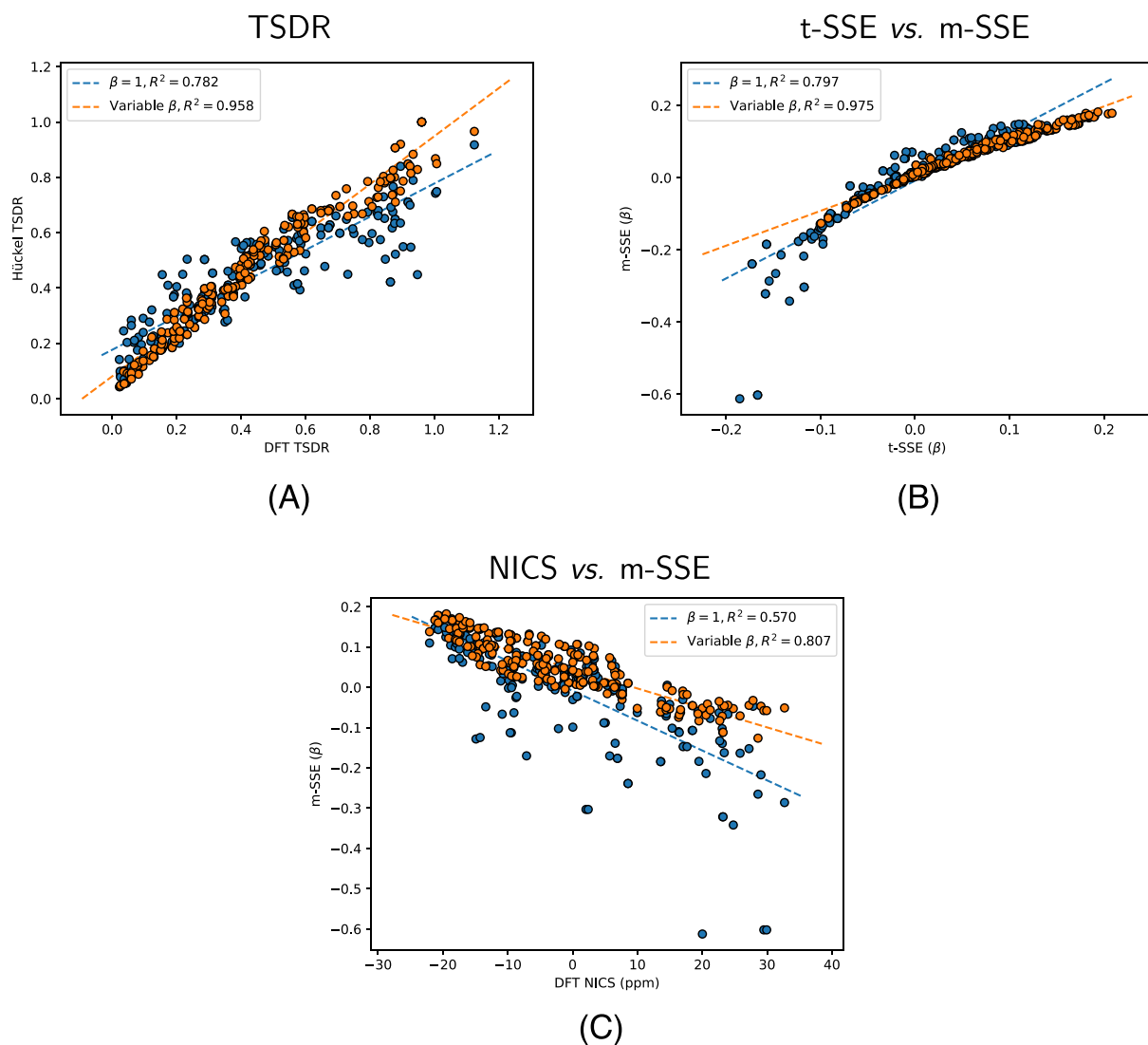

FIGURE 6 Effect of bond-length alternation on (A) total spin densities per ring, (B) m-SSE *vs.* t-SSE, and (C) NICS versus m-SSE

the order **CB-CBD** > **CB-COT** ≈ **CB-pen** (Figure 8A). Upon excitation to T_1, the central rings turn weakly aromatic, although not to the extent of their fully Baird-aromatic parents (Figure 8B). The COT ring obtains ca 65% (0.100/0.152) of the parent ring aromaticity, while the pentalene ring obtains ∼ 57% (0.055/0.097) and the CBD ring ∼ 20% (0.043/0.220). This trend is consistent with those for the FLU and HOMA aromaticity indices calculated by Ayub et al.[36] (Figures S4 and S6). By

looking at the difference in m-SSE going from S_0 to T_1 (Figure 8C), we see that the changes are dominated by the central $4n$ rings. Taken together, the difference going from S_0 to T_1 is mainly the alleviation of antiaromaticity rather than gain of aromaticity, and the Baird-aromatic character of the central ring is modest.

We can separate individual m-SSE values into contributions from circuits of different length. Figure 9 shows the contributions to the m-SSE of the central rings of **CB-**

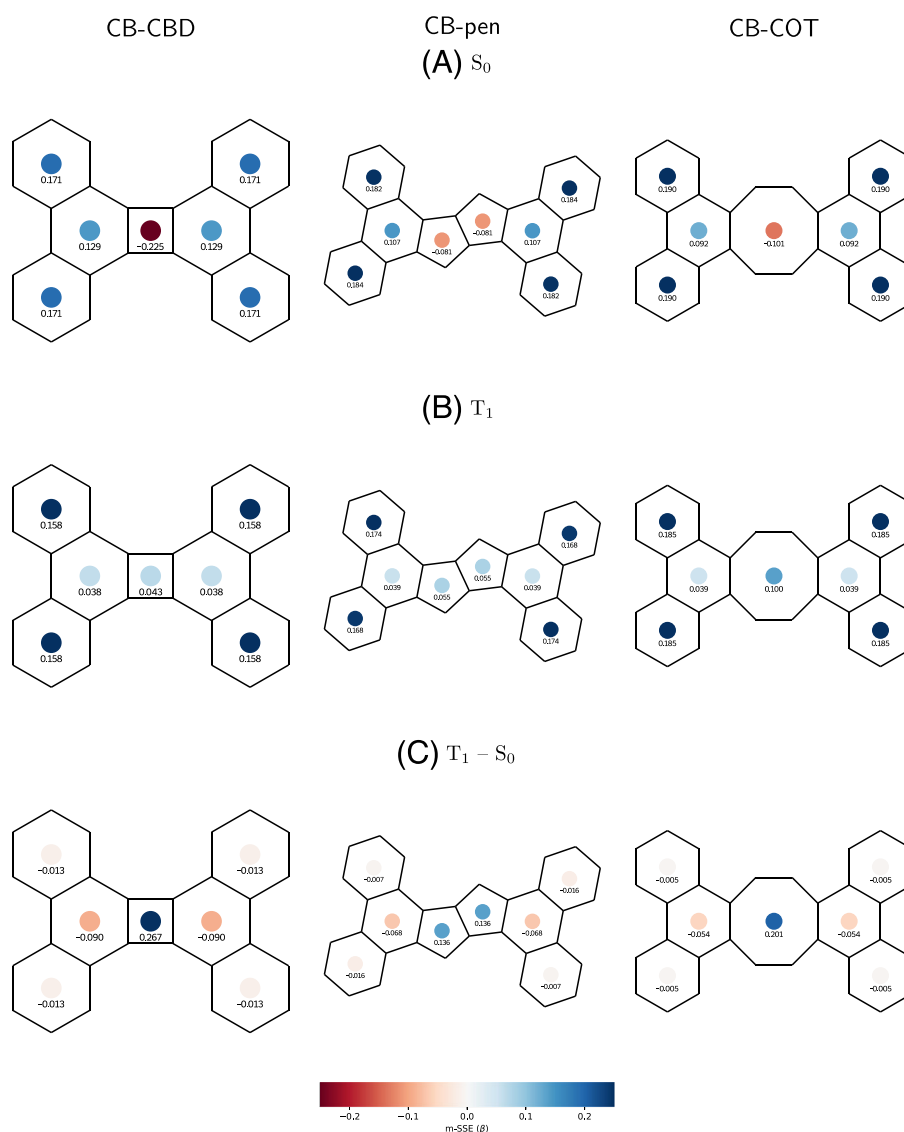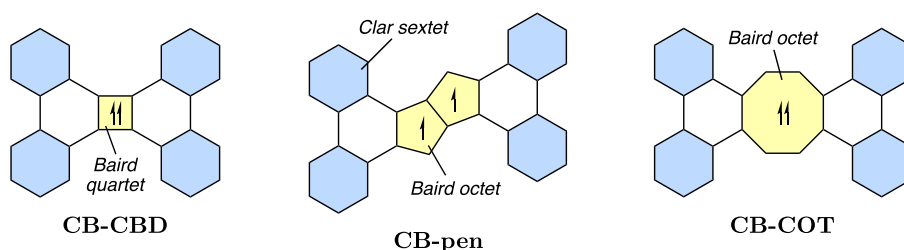**FIGURE 7** Structures that satisfy both Clar's and Baird's rules in the T_1 state

FIGURE 8 m-SSE values for **CB-CBD**, **CB-pen**, and **CB-COT** in (A) S_0, (B) T_1, and (C) the difference between T_1 and S_0. Results with the variable β method and GFN2-xTB geometries. Colored blue circles indicate the m-SSE values (darker = higher value)

CBD, **CB-Pen** and **CB-COT**, both in the S_0 and T_1 states (for **CB-Pen**, we are looking at the five-membered ring). It is clear that smaller circuits overall contribute more than larger, even though they are fewer in number. Interestingly, although the CBD ring in **CB-CBD** is weakly aromatic in T_1, it is not due to the four-membered circuit, which actually contributes a small negative CRE even in T_1. Rather, circuits with 12 and 16 atoms are responsible for the overall small positive m-SSE value (Figure 10). In contrast, the 8-membered circuits are the main contributors to the positive m-SSE value for **CB-Pen** and **CB-COT**. From the circuit analysis, it seems clear that the central ring in **CB-CBD** does not feature a localized Baird quartet.

The m-SSE can be separated into contributions not only from circuits but also orbitals, such as those from the excess α electrons in the T_1 state. As a consequence of the pairing theorem,[6] the contributions from the excess α electrons completely cancel for alternant hydrocarbons like **CB-CBD** and **CB-COT** (Figure S7). In essence, the alleviation of antiaromaticity for alternant hydrocarbons can be seen as a consequence of the removal of the effect of the "offending" electrons in the HOMO. The situation is more complex for non-alternants like **CB-pen**, where the excess α electrons do make a contribution to the m-SSE.

The m-SSE calculations showed that the variable β method based on GFN2-xTB-optimized geometries gave
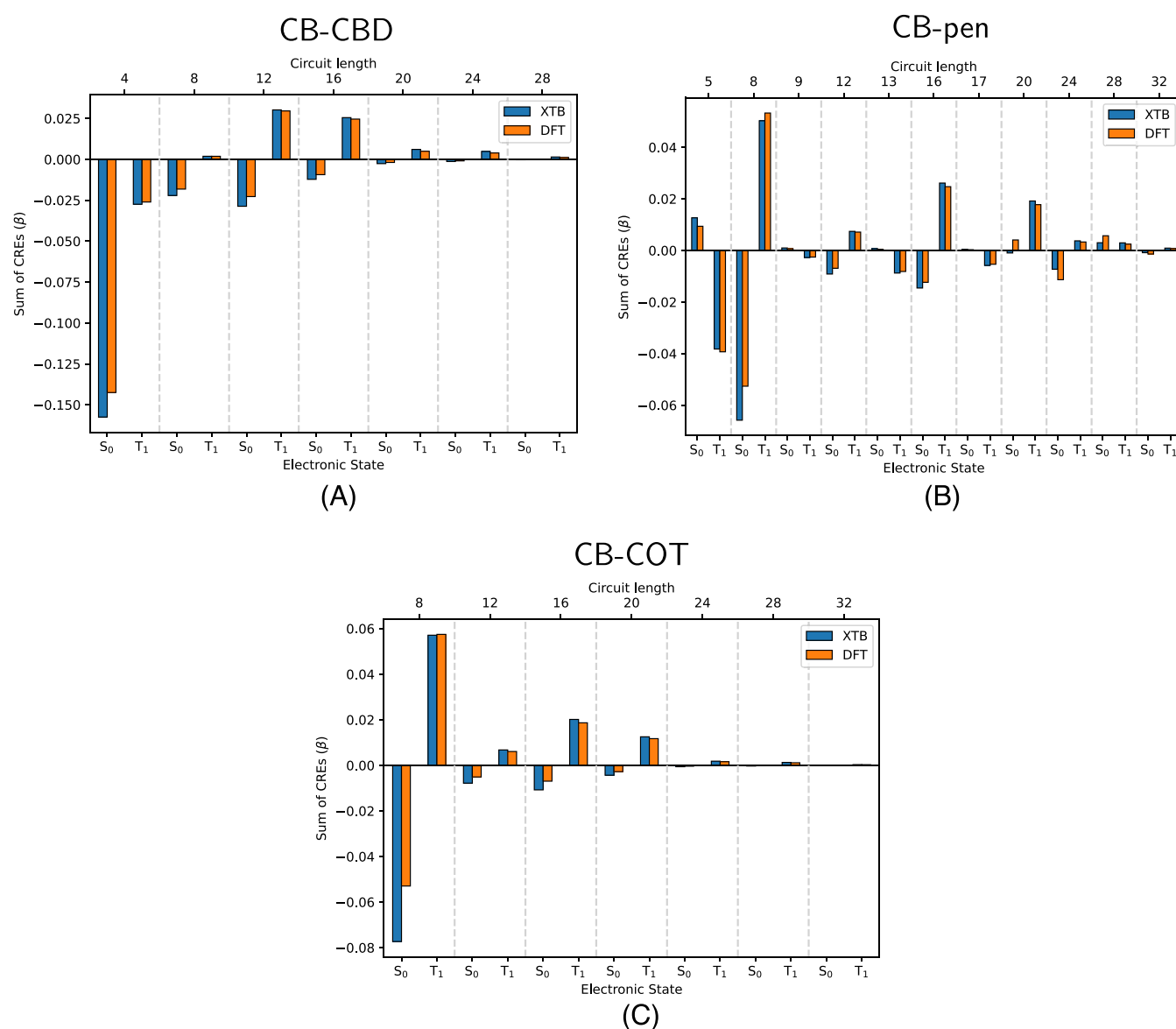

FIGURE 9 Contributions to m-SSE for central ring depending on circuit length and electronic state for (A) **CB-CBD**, (B) **CB-pen**, and (C) **CB-COT**. The value for a particular circuit length is the sum for all circuits of that length. Results with the variable β method and GFN2-xTB geometries
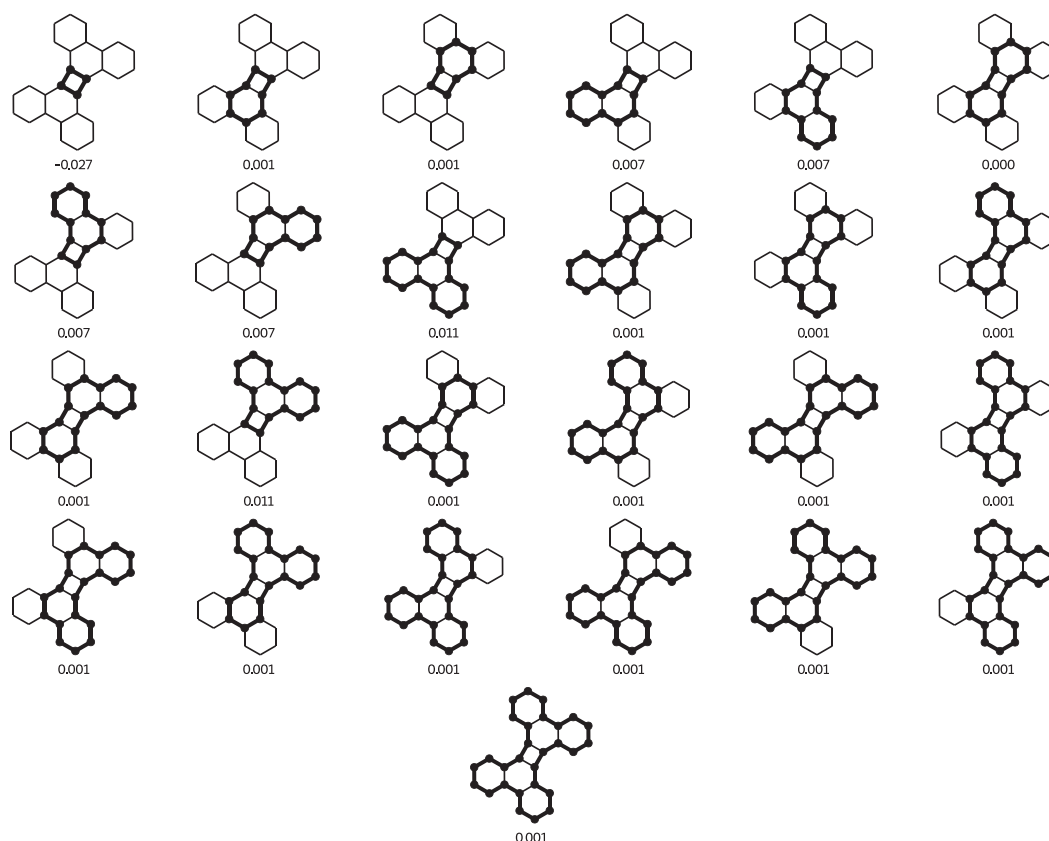
FIGURE 10 Circuits and their CRE values contributing to the m-SSE of the CBD ring in **CB-CBD** in T_1. Results with the variable β method and GFN2-xTB geometries

very similar results as for DFT geometries (Figure 9). On the other hand, using the ideal geometries with $r = 1.4 Å$ and $\beta = 1$ led to exaggerated negative m-SSE values and some numerical instabilities for pentalene (Figure S5). In contrast, the computed spin densities (Figure S8) are very similar with all three geometries and also consistent with those obtained with DFT by Ayub et al.[36]

4 | CONCLUSIONS AND OUTLOOK

We have introduced the m-SSE as a local aromaticity index that completes the set of magnetically based indices in Aihara's graph theory of aromaticity. The m-SSE was shown to correlate almost perfectly with the topologically based t-SSE index. The exception is antiaromatic rings, where m-SSE exaggerates the antiaromatic character. Introduction of bond-length alternation via the variable β method mostly resolves this problem. Potential future work could include comparisons with other local topologically based indices such as the *partial resonances energy* defined earlier by Aihara[37] and Gutman and Mizoguchi[38] or the *cyclic conjugation energy* by Gutman and Bosanac.[39]

The m-SSE (and t-SSE) was further applied to a set of *cata*-condensed PBHs in the T_1 state, showing semi-quantitative agreement with DFT-calculated NICS values. Inclusion of bond-length alternation is again crucial for capturing the effect of structural relaxation due to exciton localization. The variable β method requires both optimized geometries and pairwise parameters for each atom type. Fast geometry optimization at the GFN2-xTB level seems sufficient to capture qualitative and semi-quantitative trends as compared to reference DFT calculations. However, pairwise parameters need to be developed for other bond types than C–C. We believe that recent parametrization methods based on auto-differentiable Hückel theory would be ideally suited for this task, given that suitable reference data can be generated.

A major conceptual advantage of m-SSE over t-SSE is that it can be separated into contributions due to molecular orbitals and circuits. Analysis of a series of "Clar-Baird hybrid" molecules showed that the aromaticity of the central $4n$ ring is mainly due to relief of antiaromaticity rather than gain of Baird aromaticity. In the case of the cyclobutadiene central ring, the four-atom circuit counterintuitively contributes negatively to the m-SSE

even in T_1, and the overall slightly aromatic character of the ring is due to a number of larger circuits.

To conclude, we believe that both m-SSE and t-SSE are valuable methods for analyzing the local aromaticity of polycyclic molecules in the excited state. As the tools now become readily available to the community, we envision a renaissance for the graph theory of aromaticity.

DATA AVAILABILITY STATEMENT
Data and supporting code is available on Zenodo at https://doi.org/10.5281/zenodo.6965237; Code for the COULSON package is available on GitHub at https://github.com/kjelljorner/coulson.

ORCID
Kjell Jorner https://orcid.org/0000-0002-4191-6790

REFERENCES
[1] J. Aihara, *J. Am. Chem. Soc.* **1976**, *98*(10), 2750.
[2] I. Gutman, M. Milun, N. Trinajstic, *J. Am. Chem. Soc.* **1977**, *99*(6), 1692.
[3] W. C. Herndon, *J. Am. Chem. Soc.* **1982**, *104*(12), 3541.
[4] M. Randić, *Chem. Rev.* **2003**, *103*(9), 3449.
[5] E. Hückel, *Z. Physik* **1931**, *70*(3-4), 204.
[6] C. A. Coulson, G. S. Rushbrooke, *Math. Proc. Camb. Philos. Soc.* **1940**, *36*(2), 193.
[7] J. Aihara, *Bull. Chem. Soc. Japan* **1978**, *51*(6), 1788.
[8] J. Aihara, *Bull. Chem. Soc. Jpn.* **1987**, *60*(9), 3143.
[9] P. Ilić, B. Sinković, N. Trinajstić, *Isr. J. Chem.* **1980**, *20*(3-4), 258.
[10] N. Nishina, T. Mutai, J. Aihara, *J. Phys. Chem. A* **2017**, *121*(1), 151.
[11] J. Aihara, *J. Am. Chem. Soc.* **1995**, *117*(14), 4130.
[12] J. Aihara, *J. Chem. Soc. Faraday Trans.* **1995**, *91*(2), 237.
[13] J. Aihara, M. Makino, K. Sakamoto, *J. Phys. Chem. A* **2013**, *117*(40), 10477.
[14] J. Aihara, *Bull. Chem. Soc. Jpn.* **2004**, *77*(4), 651.
[15] J. Aihara, *Bull. Chem. Soc. Jpn.* **2018**, *91*(2), 274.
[16] J. Aihara, *J. Phys. Chem. A* **2008**, *112*(18), 4382.
[17] R. C. Haddon, *J. Am. Chem. Soc.* **1979**, *101*(7), 1722.
[18] M. Mandado, *Theor. Chem. Acc.* **2010**, *126*(5-6), 339.
[19] J. R. Dias, *J. Phys. Chem. A* **2021**, *125*(38), 8482.
[20] W. Myrvold, P. W. Fowler, J. Clarke, *Chemistry* **2021**, *3*(4), 1138.
[21] J. Aihara, *Bull. Chem. Soc. Japan* **2016**, *89*(12), 1425.
[22] N. Trinajstić, *Chemical graph theory*, CRC Press, Boca Raton **1992**.
[23] F. A. Van-Catledge, *J. Organic Chem.* **1980**, *45*(23), 4801.
[24] J. Aihara, *Chem. Phys. Lett.* **1980**, *73*(2), 404.
[25] R. Chauvin, C. Lepetit, P. W. Fowler, J.-P. Malrieu, *Phys. Chem. Chem. Phys.* **2010**, *12*(20), 5295.
[26] R. Chauvin, C. Lepetit, *Phys. Chem. Chem. Phys.* **2013**, *15*(11), 3855.
[27] F. London, *J. Phys. Radium* **1937**, *8*(10), 397.
[28] J. Aihara, *Phys. Chem. Chem. Phys.* **2016**, *18*(17), 11847.
[29] J. A. N. F. Gomes, R. B. Mallion, *Chem. Rev.* **2001**, *101*(5), 1349.
[30] J. A. Pople, K. G. Untch, *J. Am. Chem. Soc.* **1966**, *88*(21), 4811.
[31] C. Bannwarth, S. Ehlert, S. Grimme, *J. Chem. Theory Comput.* **2019**, *15*(3), 1652.
[32] C. Bannwarth, E. Caldeweyher, S. Ehlert, A. Hansen, P. Pracht, J. Seibert, S. Spicher, S. Grimme, *WIREs Comput. Mol. Sci.* **2021**, *11*(2), e1493.
[33] H. C. Longuet-Higgins, L. Salem, *Proc. R. Soc. Lond. Ser. Math. Phys. Sci.* **1959**, *251*(1265), 172.
[34] L. Z. Stolarczyk, T. M. Krygowski, *J. Phys. Org. Chem.* **2021**, *34*(3), e4153.
[35] G. Markert, E. Paenurk, R. Gershoni-Poranne, *Chem. - Eur. J.* **2021**, *27*(23), 6923.
[36] R. Ayub, O. E. Bakouri, K. Jorner, M. Solà, H. Ottosson, *J. Org. Chem.* **2017**, *82*(12), 6327.
[37] J. Aihara, *J. Am. Chem. Soc.* **1977**, *99*(7), 2048.
[38] I. Gutman, N. Mizoguchi, *Bull. Chem. Soc. Jpn.* **1990**, *63*(4), 1083.
[39] I. Gutman, S. Bosanac, *Tetrahedron* **1977**, *33*(14), 1809.

SUPPORTING INFORMATION
Additional supporting information can be found online in the Supporting Information section at the end of this article.